

# Ridge-based method for pemphigus diagnosis on immunofluorescence images\*

A.A. Dovganich, Y.A. Pchelintsev, A.V. Nasonov, A.S. Krylov, N.V. Makhneva

kryl@cs.msu.ru

Laboratory of Mathematical Method of Image Processing

Faculty of Computational Mathematics and Cybernetics

Lomonosov Moscow State University

Moscow, Russia

*In this paper, we propose a novel image processing and analysis method for immunofluorescence microscopy images of skin tissue for the problem of pemphigus diagnosis. The method includes illumination equalization algorithm, ridge detection, Euclidean distance transform, graph cut algorithm and cell boundary density metric. First four steps perform image enhancement and with last step we get numerical result. The proposed method helps the doctor find the intercellular structures both visually and numerically and make diagnosis. Experimental results for various patients show conformity between doctor's diagnosis and results of the proposed method.*

**Keywords:** Medical skin images, Pemphigus, Immunofluorescence, Ridge detection, Illumination equalization, Euclidean distance transform, Graph cut, Cell boundary density metric.

## Introduction

Nowadays image processing become more and more important in the clinic of skin diseases. New improved diagnostic methods are needed for a more thorough and accurate processing of the skin image data. Automated skin image processing has great potential to help the doctor make right diagnosis.

One of the most important problems in the diagnosis of autoimmune blistering diseases is selection of appropriate therapies, as different forms of disease require very different treatment regimens. Immunofluorescence methods [1] used in the clinic of skin diseases are the main tool in diagnosing bullous dermatoses.

Structural features obtained from immunofluorescence images can be used not only to correct diagnosis, but also to predict the further disease progression [1]. Unfortunately, in many cases, these structural features are not strong enough making it difficult to predict the disease progression. To resolve this problem we proposed a method that can improve the quality of input images and detect and analyze cell structures.

This paper is organized as follows. First we describe preprocessing step including illumination equalization [2], Gauss [3] and median filtering [4]. After preprocessing we perform ridge detection [5, 6, 7]. Then we use Euclidean distance transform [8] to find cell centers. Next cell-boundary detection using graph cut algorithm [9] is described. Then we propose cell boundary density metric. Finally we show experimental results and conclude the paper.

## Immunofluorescence image preprocessing

Preprocessing consists of 3 steps: illumination equalization, median filtering and Gauss filtering. These steps follow one after another in the sequence listing.

The work was supported by Russian Foundation for Basic Research grant 16-07-01207.

The following algorithm has been selected for illumination equalization:

1. Image is filtered by two-dimensional Gaussian filter with  $\sigma = 20$

$$G(x, y) = \frac{1}{2\pi\sigma^2} \exp\left(-\frac{x^2 + y^2}{2\sigma^2}\right)$$

So, because of big sigma we use Gaussian separable property dividing the process into two passes.

2. The original image is divided pixelwise by the Gaussian filter result with small value added to prevent division by zero. Then the result is multiplied by the average brightness of the image.
3. Median filtering is applied to delete defective pixels (due to imperfections in the matrix) and Gaussian filtering with  $\sigma = 6$  to delete thermal noise.

The results of image preprocessing are shown in Fig. 1, Fig. 2 and Fig. 3.

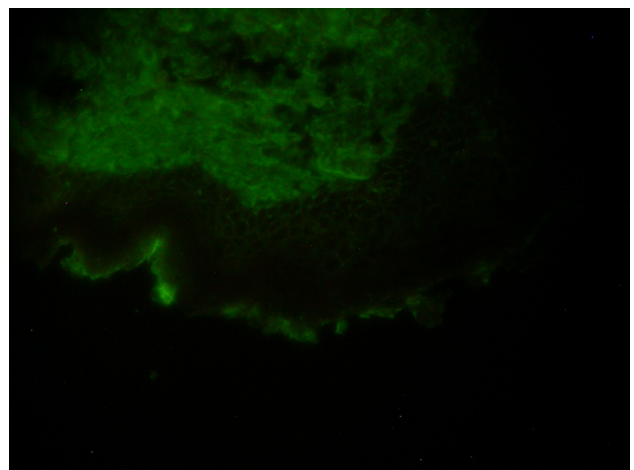


**Fig. 1.** Image of immunofluorescence microscopy before illumination equalization.

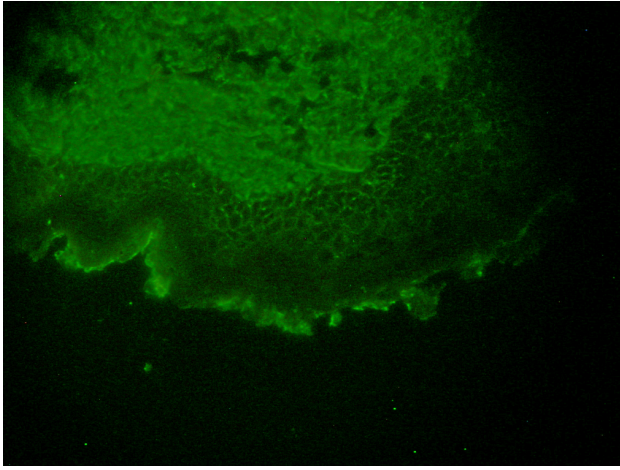


**Fig. 2.** Image of immunofluorescence microscopy after illumination equalization.

### Ridge detection

Mathematically the ridges of a smooth function of two variables are defined as a set of points that are local maxima (or minima) of the function in at least one dimension. Intercellular boundaries are typical ridges. To detect ridges we use the image with corrected illumination from the previous step. We use the following ridge detection algorithm:

1. Compute the second derivative of the image. For that we convolute the image with the second derivative of the Gaussian function with scale  $\sigma$ .
2. Construct Hessian matrix at each pixel:

$$\begin{pmatrix} L_{xx} & L_{xy} \\ L_{xy} & L_{yy} \end{pmatrix},$$

where  $L$  — values of the original image;

3. Compute the eigenvalues  $\lambda_1, \lambda_2$  of the matrix;
4. Find eigenvalue with the maximal absolute value;
5. Calculate the ratio between absolute values of the maximal eigenvalue and the minimal eigenvalue. If both eigenvalues are close to zero, then there are no features. If the ratio is greater than a threshold  $T$ , then the point is ridge. If less than the threshold but greater than zero then blob. If less than zero saddle.

We use the single scale  $\sigma = 4$  that corresponds to the real thickness of cell boundaries and imaging conditions.

The absolute value of the maximal eigenvalue is responsible for the strength of the ridge. The sign of the eigenvalue defines the polarity (ridge or valley).

The result of ridge detection algorithm is the ridge map. It contains not only intercellular structures, but also isolated structures inside cells. To delete them, we analyze the objects on the binarized ridge detection result and remove all connected objects [8] with radius less than a threshold. As a threshold select the half

maximum distance from the boundary of the cell. The binarization is carried out as follows: if we have ridge in this point of any "power", then one is written and zero otherwise.

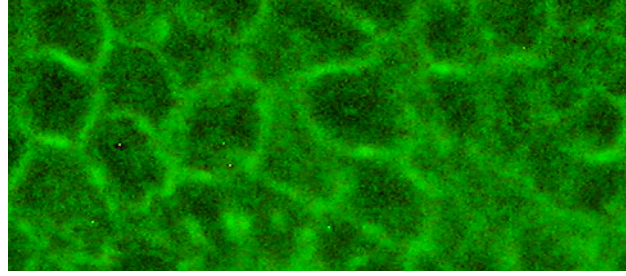


**Fig. 3.** Image of immunofluorescence microscopy after illumination equalization.

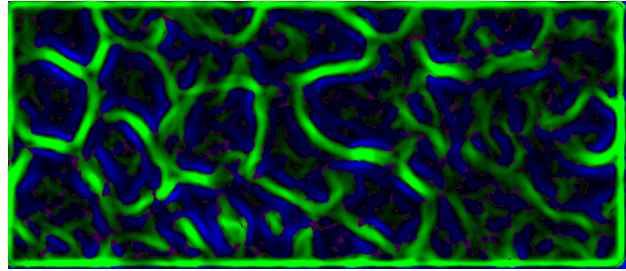


**Fig. 4.** Image of immunofluorescence microscopy after ridge detection.

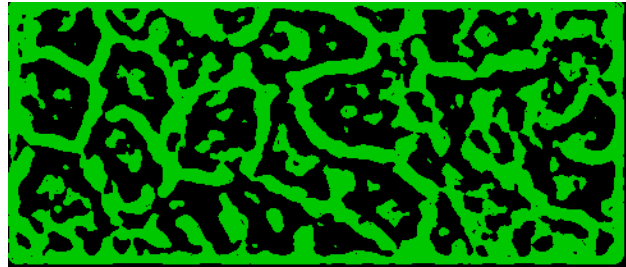


**Fig. 5.** Image of immunofluorescence microscopy after binarization.

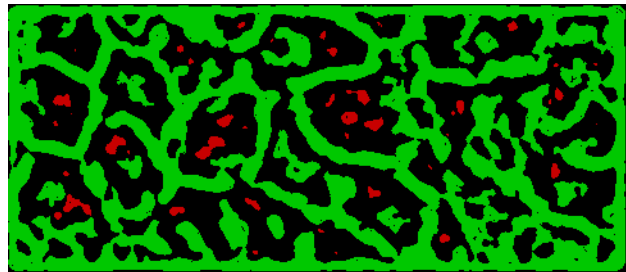


**Fig. 6.** Image of immunofluorescence microscopy after finding connected components with small radius.

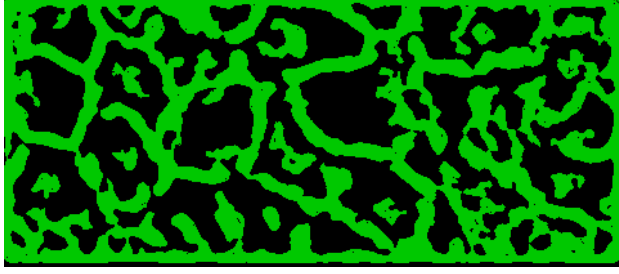


**Fig. 7.** Figure 7: Image of immunofluorescence microscopy after deleting connected components with small radius.

### Cell detection

The found cell boundaries by the ridge detection algorithm are not accurately enough for further cell boundary analysis. We use its result to detect cell centers and to apply graph cut algorithm for more accurate cell boundary detection.

We use Euclidean distance transform [9] to find cell centers. Euclidean distance or Euclidean metric is the "ordinary" (i.e. straight-line) distance between two points in Euclidean space. Distance transform is a transformation that assigns each pixel the shortest distance  $d(p, q)$  from that pixel to the object set  $O$ :

$$D(p) = \min_{q \in O} d(p, q).$$

In the case of the Euclidean distance transform, we the following distance function is used:

$$d(p, q) = \sqrt{(p_x - q_x)^2 + (p_y - q_y)^2}.$$

We compute distance map  $D$  taking the binarized ridge detection result as the object. Then we find the local maxima on the distance map. We use these points as candidates to cell centers. The candidate point is the cell center if it meets the following conditions:

1. If two cell center candidates are closer than the value in one of them on the distance map, the cell center candidate with the least distance value is removed. It is implemented by starting from the points with the highest distance value are removing all the points from its neighborhood.
2. If any of the two circles around different maxima intersect, we consider that these peaks are inside the same cell. Radius of circle are the value of distance transform in center of circle. Since the center of the cell can be only one, then we calculate its position, averaging coordinate value in the X and Y with weights proportional to the value of these maxima. This process is repeated till the center is not moving.

The result of the cell center detection is shown at Fig. 8.

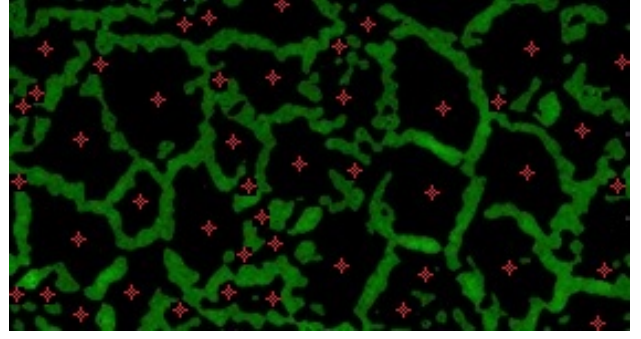


**Fig. 8.** Image of immunofluorescence microscopy containing only ridges and cell centers.

### Cell boundary detection

The main idea of the proposed cell boundary detection method is to obtain cell segmentation. Then the boundaries between them are constructed.

The unsharp masking is applied to the grayscale input image to increase the contrast level between the internal area of the cell and its boundaries.

The unsharp mask filter looks as:

$$z_{um} = z * G_{\sigma} + \alpha(z - z * G_{\sigma})$$

where  $G_{\sigma}$  is Gaussian filter,  $\sigma = 3$ ,  $\alpha = 2$ .

### Cell segmentation using graph construction and cut

At this stage each cell is analyzed separately.

An area around the cell center is considered. Its size should be large enough to contain the entire cell. At the same time it should be as low as possible to reduce computational costs and to avoid false results because of different image brightness, contrast and noise level among different areas of the image.

To restore cell boundaries the image is divided into 2 parts: cell pixels and other pixels. Chan-Vese segmentation model with only one iteration is used. Taking into account the discrete nature of the images Graph-Cut based variant is selected due to its speed and efficiency [10].

The graph of a special kind [10] is constructed for the analyzed image piece. The parameters  $\lambda_1, \lambda_2, \mu, c_1, c_2$  are selected for the whole image depending on particular equipment characteristics. The center of the cell and its small neighborhood are considered as cell inner part (objects) and are connected to the sink with infinite weight. All pixels farther from the center than a specific distance are considered as pixels outside the current cell (background) and connected with the source with infinite weight. The distance is selected based on the parameters of the photo. Remaining pixels are connected both to the source and the sink with weights defined in [10].

Then the minimal cut is searched by the algorithm from [11].



The results for different cells are combined to the single cell mask.

### Skeletonization

Next, the skeletonization of the background of the cell mask image is performed using EDT. Every pixel of the background receives the distance from it to the object (to the nearest cell). To prevent cell boundary disconnection of the external layers and to keep these cells in the skeleton, all pixels that have distance more than an average cell size become object pixels and EDT is applied again. It closes the boundaries of cells which lie in external layers of cell groups, as the new object areas lie in the external layer, and the required cells are in the internal layer.

Local maxima of distance map form the skeleton. To finish constructing the boundary non-closed contours are deleted from the result. Small unnecessary branches and added cells boundaries are removed.

### Nonadjacent cells boundary removal

As the boundaries between cells are the most important, all boundaries that are not located between adjacent cells are removed. The result of the algorithm is shown on Fig. 9.

### Cells boundary detection results

The tests were conducted with  $\lambda_1, \lambda_2, \mu, c_1, c_2$  set to 1, 1, 20000, 128 and 0 respectively [10]. With the increasing of  $\mu$  the smoothness of cells detected by Graph-Cut segmentation increases.

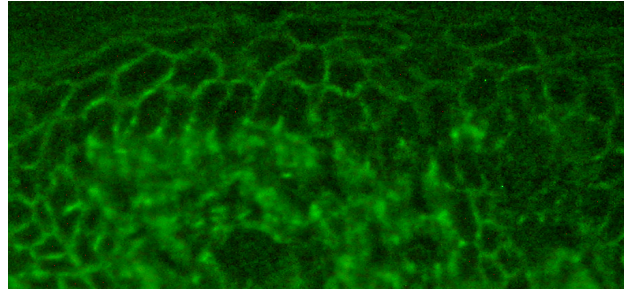
### Cell boundary analysis

We introduce cell boundary density metric to analyze cell boundary.

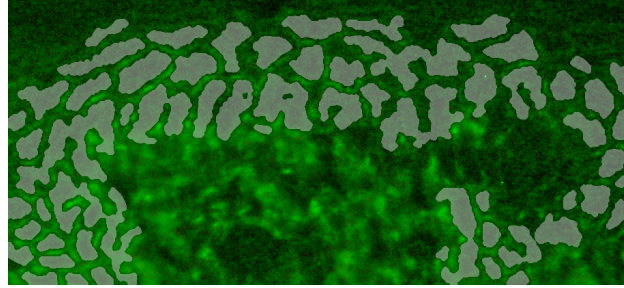
To compute cell boundary density metric we need to count the "density" between neighboring cells and then count its average value for the entire image. For this we use cell density function. It depends on the intensity of the pixel at current point. We assume that the neighboring centers are connected by series of lines connecting the two segments, perpendicular to line connection points. The length of each segment is equal to double value of the appropriate maximum on distance map. We will take only points placed on cell boundary.

"Total density" between the neighboring centers is the average density value on these lines. The total density for the entire image is the weighted sum of total density with the weights inverted proportional to the length of the lines connecting the centers. All these steps are described in general terms by the formulas below:

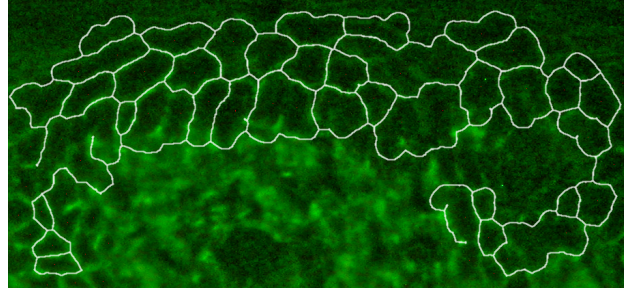
$$\begin{aligned}
 P_{line} &= P_1 + P_2 + \dots + P_n \\
 P_{center} &= \frac{P_{line1} + P_{line2} + \dots + P_{linen}}{N} \\
 P_{image} &= \frac{\frac{P_{center1}}{d_{center1}} + \dots + \frac{P_{centern}}{d_{centern}}}{N_{center}}
 \end{aligned}$$



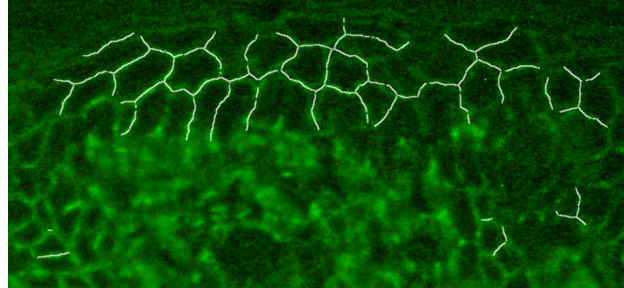
a) Source image



b) Cells detection



c) Boundary restoration



d) Final result

**Fig. 9.** Steps of the algorithm.

$P_1, \dots, P_n$  — "density" in points.

$P_{line1}, \dots, P_{linen}$  — total "density" on the lines connecting the centers of the cell line.

$N$  — the number of lines connecting the two centers.

$P_{center1}, \dots, P_{centern}$  — the average density between the centers.

$d_{center1}, \dots, d_{centern}$  — Euclidean distance from the center to the boundary.

$N_{center}$  — number of center points in the image.

$P_{image}$  — total boundary density for the entire image (cell boundary density metric).

High cell boundary density metric value corresponds to intensive cell boundaries. If the metric value is

small, it can be assumed that cell boundary is dotted. High metric value is also typical to normal cell grid with the presence of pellets. They are the brightest structures that have a huge contribution to the total image "density" value.

## Results

We have evaluated the proposed method with real immunofluorescence images of pemphigus taken from different patents diagnosed by a doctor.

The Table 1 presents the experimental results. The first column contains the calculated cell boundary density metrics value. The second one is the classification of cell structures made by a doctor after image enhancement. The last one is the disease progression.

Boundary metric	Intercellular structures	Disease progression
6,99	Grid	Favorable
7,32	Dotted grid, Pellets	Adverse
4,25	Grid	Favorable
7,94	Pellets	Adverse
4,95	Grid	Favorable
6,53	Grid	Favorable
8,65	Grid, Pellets	Adverse
4,95	Grid	Favorable
7,03	Grid	Favorable
1,50	Grid	Favorable
8,19	Grid	Favorable
5,66	Grid	Favorable
5,79	Grid	Adverse
7,09	Grid	Favorable
6,88	Grid	Favorable
6,09	Grid, Dotted grid	Favorable
6,80	Grid	Favorable
5,72	Dotted grid	Favorable
2,56	Grid	Favorable
6,99	Grid	Favorable
3,79	Grid	Favorable
7,29	Grid, Pellets	Adverse
5,82	Dotted grid	Favorable
7,95	Grid, Pellets	Favorable
6,20	Grid	Favorable
6,24	Grid	Favorable
4,70	Grid	Favorable

**Table 1.** Experimental results.

## Conclusion

We have proposed an image processing and analysis algorithm for the images of immunofluorescence microscopy of pemphigus. The algorithm calculates cell boundary density metric based on the structural features of intercellular boundaries. The proposed algorithm has been tested with real images of immunofluorescence microscopy. Experimental results for various

patients demonstrate that the proposed method can be used as a pemphigus diagnostic tool.

## References

- [1] *Мажнева Н. В., Белецкая Л. В.* Иммунофлюоресценция в клинике аутоиммунных буллезных дерматозов // Издательство "Академия Естествознания", 2010 год.
- [2] *Лукин А.С.* Введение в цифровую обработку сигналов Учебное пособие Факультета ВМК МГУ, 54, 2007.
- [3] *Babaud J., Witkin A. P., Baudin M., Duda R.* Uniqueness of the Gaussian kernel for scale-space filtering // Pattern Analysis and Machine Intelligence, pp. 26–33, 1986.
- [4] *Brownrigg D. R. K.* The weighted median filter // Magazine Communications of the ACM, pp. 807–818, 1984.
- [5] *Damon J.* Properties of ridges and cores for two-dimensional images // Journal of Mathematical Imaging and Vision, pp. 163–174, 1999.
- [6] *Eberly D., Gardner R., Morse B., Pizer S. C.* Ridges for image analysis // Journal of Mathematical Imaging and Vision, pp. 353–373, 1994.
- [7] *David E.* Ridges in Image and Data Analysis // Computational imaging and vision 7, 228 p., 1996.
- [8] *Shapiro L., Stockman G. C.* Computer Vision // ed: Prentice Hall, pp. 69–73, 2001.
- [9] *Fabbri R. et al* 2D Euclidean distance transform algorithms: A comparative survey // ACM Computing Surveys (CSUR). Vol. 40. No. 1, 2008.
- [10] *Danek O. et al* Smooth Chan-Vese segmentation via graph cuts // Pattern Recognition Letters. Vol. 33, No. 10, pp. 1405–1410, 2012.
- [11] *Boykov Y., Kolmogorov V.* An experimental comparison of min-cut/max-flow algorithms for energy minimization in vision // IEEE Transactions on Pattern Analysis and Machine Intelligence, Vol. 26, No. 9, pp. 1124–1137, 2004.

## About the authors

Andrey A. Dovganich, master student at Faculty of Computational Mathematics and Cybernetics, Lomonosov Moscow State University (CMC MSU).

Yakov A. Pchelintsev, bachelor student at CMC MSU.

Andrey V. Nasonov, Dr, senior researcher at CMC MSU. E-mail: nasonov@cs.msu.ru

Andrey S. Krylov, Prof, Head of the Laboratory of Mathematical Methods of Image Processing at CMC MSU. E-mail: kryl@cs.msu.ru

Natalia V. Makhneva, Prof, Doctor of Medical Sciences MF Vladimirsky Moscow Reg Sci Res Clin Univ. E-mail: makhneva@mail.ru